COMPUTATIONAL MECHANICS 2021
36th conference with international participation
Srní
November 8 - 10, 2021

Influence of mesh density on the analysis of textured journal bearings

J. Rendl, L. Smolík

NTIS – New Technologies for the Information Society, Faculty of Applied Sciences, University of West Bohemia, Univerzitní 8, 301 00 Plzeň, Czech Republic

The stability of a rotating system supported on a journal bearing can be improved by suitable texturing of the bearing shell. This contribution focuses on mathematical modelling of a textured bearing using the finite difference method and the study of mesh density impacts on static analysis results and estimated stability thresholds.

A simple 2 DoF rotor-bearing model with various texture layouts is analysed. Textures in all considered layouts are located in the replaceable bottom bearing shell to emphasise the influence of the texturing on the system stability compared to the plain bearing. The investigated texture layouts are depicted in Fig. 1a–d. The texture consists of dimples in regular grid (1 mm grid gap) produced by mechanical indentation with a steel ball of 1 mm diameter. The measured dimple profile is shown in Fig. 1e. Investigated bearing was designed with these parameters: inner diameter 37.933 mm, bearing length 20 mm and radial clearance 55 μm. Bearing is supplied by oil with dynamic viscosity 14 mPa.s through the circular bore of 5 mm diameter.

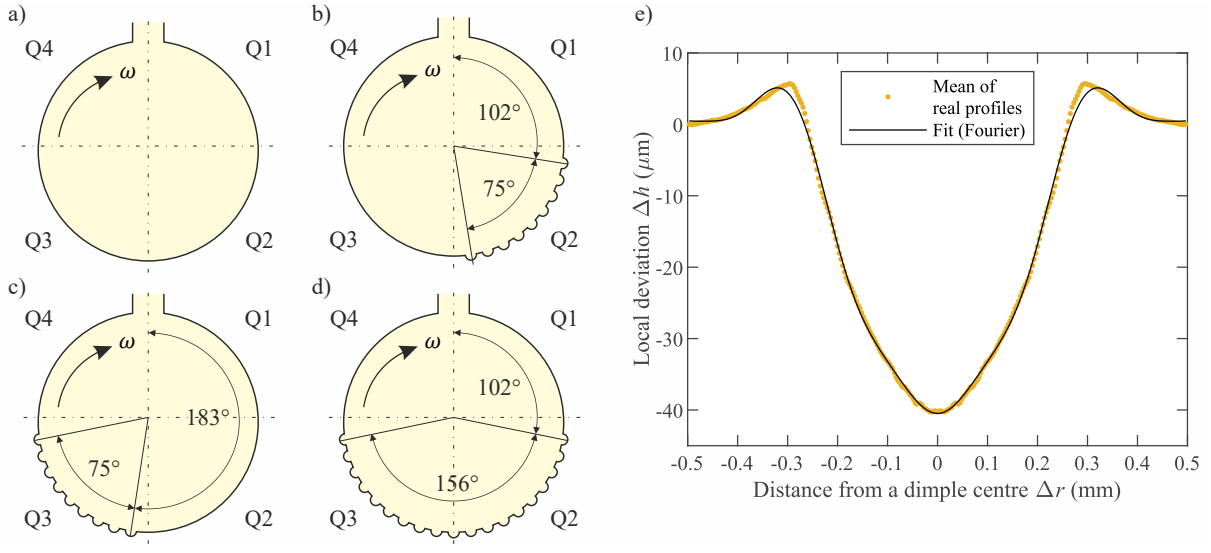

Fig. 1. Investigated bearing layouts: a) plain bearing, b) layout Q2 (26×19 dimples), c) layout Q3 (26×19 dimples), d) layout Q23 (53×19 dimples), e) measured dimple profile

The Reynolds equation [1, 4] governs the pressure field generated in a laminar flow of isoviscous incompressible Newtonian fluid. The film height is a sum of nominal gap h_{nom} of cylindrical bearing and local deviation Δh due to texture. The finite difference method [1] was employed in an in-house software for pressure field calculation and the hydrodynamic force

evaluation. The stability threshold speed assessment is then performed using the Routh-Hurwitz criterion described in [1].

The results of numerical simulations are affected by the utilised cavitation modelling approach and chosen computational mesh density defined as the number of nodes per mm^2. A mass-conserving cavitation modelling [3] approach (Elrod equation) is unsuitable for dense computational meshes because of memory restriction in regular workstations. The static equilibrium points calculated by utilising the Gümbel condition (G), which violates the conservation of mass [1, 4], are compared with those calculated using the mass-conserving Elrod equation (E) in Fig. 2a. Layout Q2 is used for the presented simulations. An in-house software solver uses a direct solution (Dir) for pressure field calculation and the Gümbel cavitation condition due to memory access restrictions. For verification of the obtained results, commercial software AVL Excite was used. This software employs the finite difference method and has a native multi-grid solver (MG) for pressure field solution with both Gümbel and Elrod cavitation models. Unfortunately, the total number of nodes for the numerical solution of the Elrod equation is restricted to ca. 4×10^5, which corresponds with the mesh density of 13×13 nodes per mm^2.

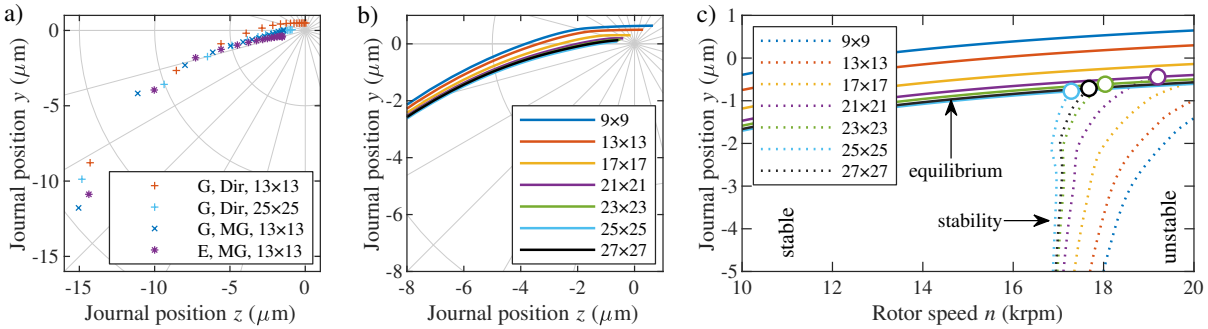

Fig. 2. Loci of equilibrium points for layout Q2: a) various numerical algorithms, b) various mesh densities, and c) threshold speeds (intersections of loci of equilibrium points with stability borderline denoted by ○) for various mesh densities; mesh density given in nodes per mm^2

The equilibrium points differ at higher eccentricities more significantly because of the numerical method rather than the cavitation model. The cavitation model influences the equilibrium points at lower eccentricities, but the results obtained on a dense mesh with the Gümbel condition are similar to the results of the mass-conserving cavitation model. Figs. 2b–c show the results calculated using the in-house software and various mesh densities from 9×9 to 27×27 nodes per mm^2. It is demonstrated on the static equilibrium points Fig. 2b and detected threshold speeds denoted by circles (intersection of equilibrium points and stability borderline) in Fig. 2c that coarse computational meshes predict different results. The results start to converge to limit values with the mesh density around 23×23 nodes per mm^2. Final mesh density 25×25 nodes per mm^2 was established as optimal concerning both computational accuracy and computational time costs.

Static equilibrium points for various texture layouts, bearing loads and relative supply pressures are depicted in Fig. 3. The textures in the third quadrant (layouts Q3 and Q23) affect the loci more significantly with the increased bearing load. However, the differences are also apparent for the lower nominal load. This behaviour is caused by the location of both texture and load-carrying pressure field in the third quadrant. On the contrary, the equilibrium points obtained for layout Q2 are almost at the same positions as in the plain journal bearing.

Threshold speeds for instability, which are deduced from linearised stiffness and damping coefficients in static equilibrium points, are compared in Fig. 4. Vertical axes in the individual

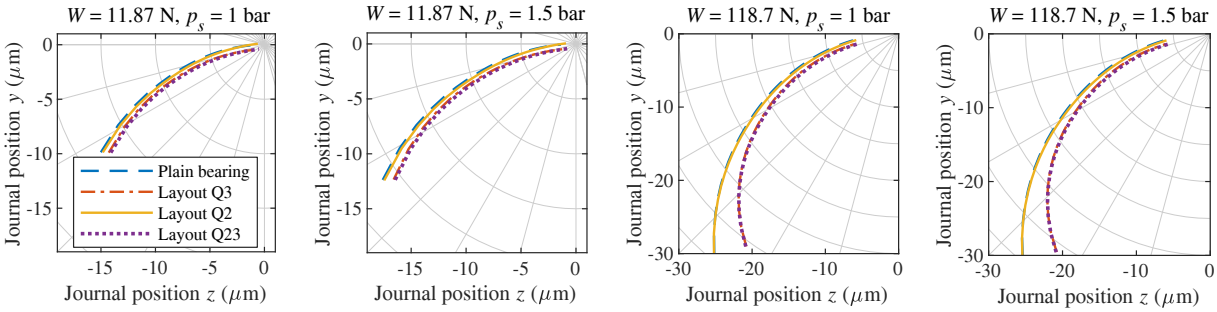

Fig. 3. Loci of equilibrium points for variou texture layouts, bearing loads and relative supply pressures

subfigures are depicted in a logarithmic scale for better clarity. The textures located in regions with high pressure gradients significantly impact the threshold speed in the case of lightly-loaded bearings. The threshold speed is then shifted from 17 krpm for the plain bearing to 19.7 krpm for layout Q2 and out of investigated speed range (i.e., above 20 krpm) for the case of layout Q23. On the other hand, threshold speed shifts only negligibly when the texture is located in the second quadrant of the lightly-loaded bearing. The differences between all layouts are also negligible when higher static load (0.15 MPa) is applied.

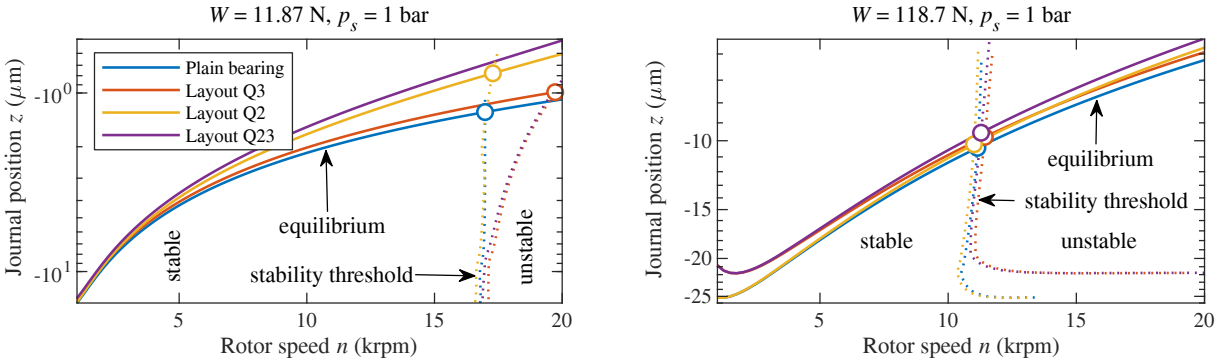

Fig. 4. Comparison of estimated threshold speeds for various texture layouts and bearing loads

Acknowledgements

This publication was supported by project SGS-2019-009 of Czech Ministry of Education, Youth and Sport. Results verification would not be possible without the AVL Excite software, which is available in the framework of the University Partnership program of AVL List GmbH and whose usage is greatly acknowledged.

References

[1] Dyk, Š., Rendl, J., Byrtus, M., Smolík, L. Dynamic coefficients and stability analysis of finite-length journal bearings considering approximate analytical solutions of the Reynolds equation, Tribology International 130 (2019) 229-244.

[2] Gropper, D., Wang, L., Harvey, T.J., Hydrodynamic lubrication of textured surfaces, Tribology International 94 (2016) 509-529.

[3] Qiu, Y., Khonsari, M. M., On the prediction of cavitation in dimples using a mass-conservative algorithm, Journal of Tribology 131 (4) (2009) No. 041702.

[4] Stachowiak, G. W., Batchelor, A. W., Engineering tribology, 4th edition, Butterworth-Heinemann, St. Louis, USA, 2013.